ELSEVIER

Journal of Nuclear Materials 246 (1997) 70–76

journal of nuclear materials

Correlations between the electrochemical behaviour and surface film composition of TZM alloy exposed to divertor water coolant environments [1]

Marie-Françoise Maday *, Rossella Giorgi, Theodoros Dikonimos-Makris

ENEA-CRE-Casaccia, Dipartimento Innovazione, Divisione Nuovi Materiali, P.B. 2400-00100, Rome, Italy

Received 28 March 1996; accepted 3 March 1997

Abstract

X-ray photoelectron spectroscopy (XPS) has been carried out on TZM alloy surfaces after short and long immersion tests in high temperature (250°C) aqueous environments simulating possible fusion reactor coolant conditions during operation. Phase identification by XPS was used in connection with the open circuit potential trends to suggest plausible hypotheses about TZM corrosion behaviour in the various chemical environments considered in this study. It was proposed that exposure of TZM to oxidizing water conditions produced poorly protective layers, which consist essentially of low (IV) and intermediate (V) valency Mo oxides/hydroxides. Conversely the results obtained in deaerated and reducing water conditions suggested that barrier films could develop in these environments: the phases exhibit a bilayered structure and consisted of an inner tetravalent Mo oxide/hydroxide and an outer hexavalent Mo oxide. The protective properties of such layers were attributed to the hexavalent Mo species. © 1997 Elsevier Science B.V.

1. Introduction

Molybdenum alloys have been considered as possible materials for the cooling structures of the high heat flux components in fusion reactors. The objective of an earlier investigation [1,2], carried out in the frame of the European Technology Programme, was to study the low cycle fatigue (LCF) performances of the Mo low alloyed version, TZM (Metallwerk Plansee, Austria), in high temperature water, either deaerated or containing separate additions of oxygen, hydrogen and hydrogen peroxide, in order to simulate various chemical environments of the coolant inside the divertor channels during reactor operation.

In an attempt to explain the fatigue life dependence on environmental and stress factors, hypothetical cracking mechanisms were proposed [1,2], taking into account the results of fractographic observations and the behaviour of the open circuit potentials, which were continuously recorded during testing. These last data were used in combination with visual assessments of the outer specimen area aspects, to draw conclusions about TZM surface state properties after exposure to the various environments, which correlate reasonably with the proposed models, but remained questionable as far as they are not supported by surface analysis. Such evaluations were subsequently performed by X-ray photoelectron spectroscopy, on samples exposed to the environments during LCF testing.

In this paper, the results of XPS measurements are presented and discussed in relation to the open circuit potential behaviour found experimentally.

2. Experimental details

Surface preparation of TZM (chemical composition in wt% [3]: Mo: 99.369, Ti: 0.5, Zr: 0.08, C:0.025, H: 0.0005, O: 0.025, N: 0. 0005) flat specimens for exposure to the LCF testing environments was carried out by wet

* Corresponding author. Tel.: +39-6 3048 4391; fax: +39-6 3048 3327.

[1] This work has been carried out in the frame of the European Fusion Technology Programme.

PII S0022-3115(97)00020-2

grinding on a 20 μm diamond disk and final polishing with diamond pastes up to 1 μm on nylon and silk laps. The samples were cleaned in acetone, before being introduced on the autoclave bottom on an insulating support. The required deaerated, oxygenated and hydrogenated water chemistries ($O_2 < 10^{-8}$ M/l, $O_2 = 10^{-5}$ M/l, $H_2 = 10^{-3}$ M/l, respectively) were ensured over the entire test duration by means of automatically controlled flows of appropriate gas or gas mixtures through the water in the storage tank of the recirculating loop. Conversely, the occurrence of significant decomposition of hydrogen peroxide at 250°C did not allow to keep constant the level of this species in the testing solution. A working concentration range between 2.10^{-4} and 2.10^{-5} M/l was, therefore, established and maintained by periodical injecting, specific contents of H_2O_2 to the feedwater. Exposure times of the samples were dictated by the fatigue lives of the LCF specimens, which depend on environmental as well as on stress factors. The values reported in Tables 1 and 2 for each sample designation, indicate that longer immersion times were associated with the LCF tests performed under the lower load amplitude which induced lower strain and gave rise to extended fatigue lives. TZM corrosion potentials were continuously recorded during the tests against an Ag/AgCl reference electrode and converted into the standard hydrogen scale (SHE).

After testing, the samples were transferred for XPS studies in containers under air exposure. For technical reasons, the time elapsed between the removal from the autoclave and introduction in the UHV chamber for surface analysis of the specimens exposed to the short term tests was significantly longer than that relative to the long-term experiments. XPS analysis were performed by using a VG ESCALAB MKII spectrometer, at the base pressure of 10^{-9} mbar. Mg Kα radiation at 1253.6 eV was employed as excitation source. Detailed spectra of Mo 3d, O 1s and Ti 2p were acquired at 20 eV analyzer pass energy, which resulted in an effective resolution of 1 eV on the Ag $3d_{5/2}$ peak. The energy scale was calibrated against Au $4f_{7/2}$ at 84.05 eV and Cu $2p_{3/2}$ at 932.4 eV. Curve fitting was performed to separate into their different valency states the Mo 3d signals, resulting from the overlapping of the various Mo species contributions, which were shifted by values ranging from 1.6 to 4.8 eV with respect to the metallic state, and were split into the doublet $3d_{5/2,3/2}$ separated by 3.1 eV. A symmetrical Gaussian/Lorentian mixed product function was used to fit these peaks after a linear background subtraction according to Shirley [4]. Measurements were taken at two different take-off angles (normal and grazing) in order to sample different depths.

3. Experimental results

The main experimental features resulting from the tests and relevant for the present investigation are summarized in Tables 1 and 2 for each sample designation. It could be seen that the TZM potential evolved anodically in deaerated and hydrogenated water, but remained constant at more cathodic values in the oxygenated aqueous environment. The trend reported for the hydrogen peroxide solution was relative to a typical chemistry transient, during which H_2O_2 varied from 2.10^{-4} to 2.10^{-5} M/l and was reproducible throughout the testing period.

Platinum voltages are reported in Table 3 as a function of water chemistry and related equilibria, which are expected to determine the redox character of the environment.

XPS analysis carried out on the exposed sample surfaces revealed the presence of Mo oxides with more than one valency, whose relative amounts were evidenced by Mo 3d peak deconvolution. All the spectra were deconvoluted in four doublets; their intensities and separations were in agreement with the theoretical values predicted for the spin orbit splitting; each doublet was representative of a specific oxidation state. An example of a typical curve fitting, obtained for specimen M11, is shown in Fig. 1. In reasonable agreement with literature data [5–8], peaks denoted A1 (the $3d_{5/2}$ component centred at 228.1 ± 0.1

Table 1
Experimental features relative to the TZM samples exposed during the LCF tests at 20 kN load amplitude in 250°C water environments

Environments	Specimen designation	Exposure times (h) 20 kN load	Open circuit potential, ΔE_{oc} (V versus SHE [a])	Outer surface aspect
Air	M0	55	–	silvery white
Deaerated H_2O	M1	42	−0.38, −0.32	light purple
$H_2O + 10^{-3}$ M/l H_2	M2	33	−0.4, −0.22	light brown to yellowish
$H_2O + 10^{-5}$ M/l O_2	M3	59	−0.46	purple–black scale
$H_2O + 10^{-4}$–10^{-5} M/l H_2O_2	M4	28	−0.36– −0.46	loose, black deposit, underlying matrix corroded

[a] In volts versus the standard hydrogen electrode.

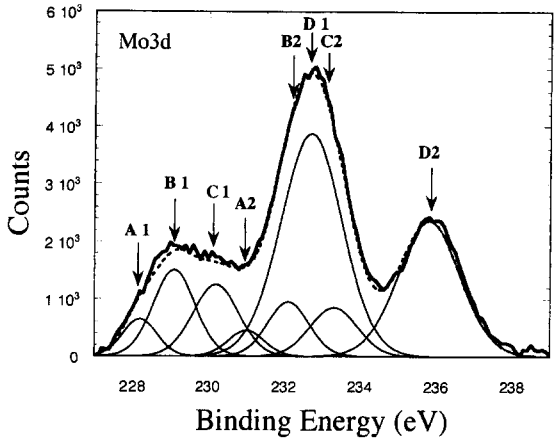

Fig. 1. Mo 3d peak for sample M11 showing the deconvoluted components: A1–A2 represents the spin orbit doublet (5/2, 3/2) for the Mo(0) state; in the same way, B1–B2 and C1–C2 are representative of the Mo(IV) valence in MoO_2 and $MoO(OH)_2$, respectively; peaks D1–D2 are for Mo(VI). Dashed and thick curves represent the sum of the individual components and the experimental data, respectively.

eV and with a FWHM of 1.2–1.4 eV and A2 were attributed to Mo(0), while the other three doublets, labelled B, C and D, were ascribed to Mo(IV) in MoO_2, Mo(IV) in the oxyhydroxide $MoO(OH)_2$ and Mo(VI) in MoO_3 and/or the hydrated form H_2MoO_4; their $3d_{5/2}$ components, B1, C1 and D1, were centred at 229.1 ± 0.1 eV (FWHM 1.3–1.6 eV), 230.2 ± 0.1 eV (FWHM 1.4–1.7 eV) and 232.5 ± 0.2 eV (FWHM 1.8–2.1 eV), respectively. The FWHM of all the species and especially of Mo(VI), were larger than those of their relative standards reported in the literature. These findings could be attributed either to the coexistence of several overlapping components, or to the contribution of polyhydrated forms of the oxides, whose XPS reference data are not available in the literature.

Surface films were shown to consist mainly of tetravalent molybdenum (reported as dehydrated MoO_2 and hydrated $MoO(OH)_2$) and hexavalent molybdenum (MoO_3 or H_2MoO_4). The presence of pentavalent Mo was also hypothesized on the specimens exposed to hydrogen peroxide solution, since a component at an energy between the values attributed to Mo(IV) and Mo(VI) was needed to fit the relative Mo 3d spectra. Tetravalent titanium oxide was found in the layers formed in all the testing environments, whereas Zr was never detected.

As previously mentioned, these spectra resulted from the overlapping of several lines; the main peak itself contained, at least, three components, arising from the contribution of different chemical species and spin-orbit doublets. Signals from individual Mo valent states were,

Table 2
Experimental features relative to the TZM samples exposed during the LCF tests at 17 kN load amplitude and in 250°C water environments

Environments	Specimen designation	Exposure times (h) 17 kN load	Open circuit potential, ΔE_{oc} (V versus SHE [a])	Outer surface aspect
Deaerated H_2O	M11	100	−0.39, −0.28	yellowish-blue
$H_2O + 10^{-3}$ M/l H_2	M22	94	−0.42, −0.22	light brown to yellowish
$H_2O + 10^{-5}$ M/l O_2	M33	117	−0.44	purple–black scales with loose, thin black deposit
$H_2O + 10^{-4}$–10^{-5} M/l H_2O_2	M44	147	−0.38– −0.48	black friable deposit, underlying matrix corroded

[a] In volts versus the standard hydrogen electrode.

Table 3
Experimental and theoretical open circuit potential values of platinum electrode in the testing water environments at 250°C [2]

Environment	Measured Pt potential (initial) (V versus SHE *)	Dominant redox couples and relative potential determining reactions	Theoretical equilibrium potentials at 250°C (V versus SHE [a])
Deaerated water	−0.26	H_2O/H_2, $2e^- + 2H_2O = 2OH^- + H_2$	$-0.0518 \log PH_2 - 0.1037pH = -0.3$
Water + $10^{\pm 3}$ M/l H_2	−0.52	H^+/H_2, $2e^- + 2H^+ = H_2$	$-0.0518 \log PH_2 - 0.1037pH = -0.55$
Water + 10^{-5} M/l O_2	0.26	O_2/H_2O, $2e^- + 1/2O_2 + 2H^+ = 2\,H_2O$	$1.049 + 0.0259 \log PO_2 - 0.1037pH = 0.42$
Water + H_2O_2 2.10^{-4}–2.10^{-5} M/l	0.20 ÷ 0.08	H_2O_2/H_2O, $2e^- + 2(OH)_{ads} = 2OH^-$	$(\Delta E_{250°})_{SHE}$ [b] $- 0.1037pH < 0.3$ (extrapolated at saturation)

[a] In volts versus the standard hydrogen electrode.
[b] Standard potential at 250°C of reaction: $2e^- + 2(OH)_{ads} = 2OH^-$, not reported in literature.

nevertheless, identified in specific energy intervals and were selected to follow the evolution of the corresponding species. These intervals, bonded in Fig. 2 by the shaded areas, include the following transitions: the Mo $3d_{5/2}$ from metallic Mo, the Mo $3d_{5/2}$ from tetravalent Mo oxide, the Mo $3d_{3/2}$ from hexavalent Mo oxide. The oxide film chemistry relative to each testing environment appeared to vary with exposure time in the following manner:

— Prolonged immersion times in deaerated water produced moderate film thickening, as shown by the slight decrease of the Mo(0) signal at the lowest energy, while the increase of the signal at the highest energy denoted a progressive enrichment of the layer with hexavalent Mo. Moreover, a comparison of the spectra collected at normal and grazing take-off angles on specimen M11 (Fig. 3), revealing the enhancement of the Mo(VI) contribution and the attenuation of the lower oxidation state signal as the sampling depth decreased, indicated that the oxide has developed according to a bilayered morphology (namely: inner Mo(IV), outer Mo(VI)). The apparent lack of this ordered structure at shorter exposure time, suggested by the invariance of the spectra acquired at different take-off angles, could be related to an incomplete surface coverage with MoO_3.

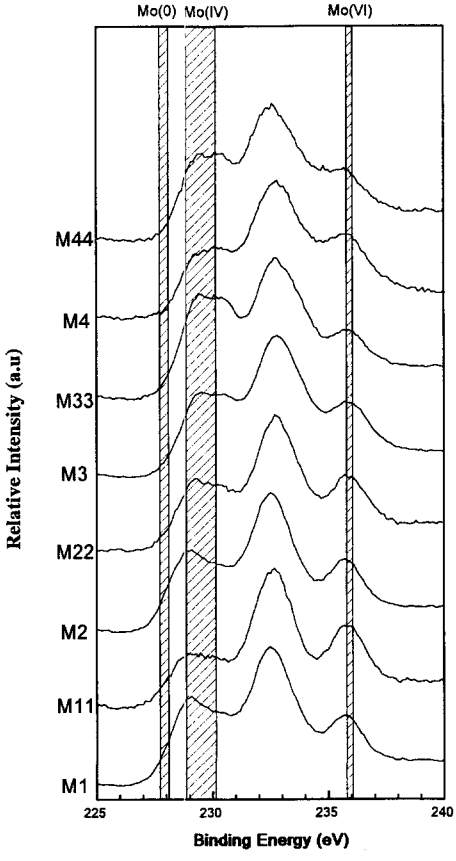

Fig. 2. Mo 3d spectra of the TZM samples reported in Table 1Table 2. The shaded areas represent the energy intervals where peaks from Mo(0), M0(IV) and Mo(VI) species alone are falling.

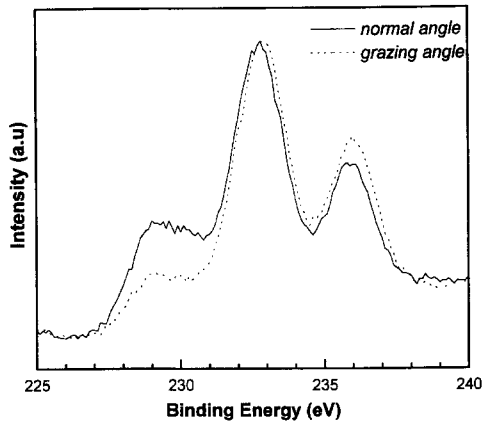

Fig. 3. Mo 3d spectra for sample M11, collected at two different take-off angles.

— Even though a similar trend occurred in hydrogenated environment, it was far less pronounced and gave the idea that a steady bi-layered oxide state was already formed during the short immersion test.

— Continued exposure of TZM to water containing 10^{-5} M/l dissolved oxygen did not lead to substantial film growth, as it appeared from the constancy of the Mo(0) signal in the spectra of specimens M3 and M33. The compositional change of the layer with immersion time consisted in an increase of the Mo(IV)/Mo(VI) ratio.

— The total absence of the peak relative to metallic molybdenum from specimens M4 and M44 surface analysis, denoted that the film formed in hydrogen peroxide solutions was very thick, even after the shorter immersion test. The evolution of the different valency molybdenum signals indicated that the relative amount of tetravalent Mo in the layer increased with exposure time, while that of pentavalent Mo remained constant.

— Tetravalent Ti contribution to the total spectra from the films produced in deaerated, oxygenated and hydrogenated water, did not vary with the contact time. Quantitative calculations using the integrated intensities of the peaks relative to the various cationic species indicated that the amount of Ti in the layer reflected approximately that of the substrate (about 1 at.%). A higher concentration of this component was conversely found in the oxide formed under the short immersion test in hydrogen peroxide solution, but the content returned to the bulk alloy value after longer exposure to this environment.

4. Discussion

Information about the stability in water at various temperatures of the solid and dissolved compounds deriv-

ing from Mo aqueous corrosion [9], requires the knowledge of their Gibbs energies, which is actually incomplete. For instance, the potential-pH diagrams, which have been established for the Mo/H_2O system at temperatures up to 300°C [10], do not include all the possible species, for the lack of their relative thermodynamical quantities in the available literature. An extrapolation of the theoretical results reported in Ref. [10] to the case of TZM, which contains essentially molybdenum and is expected to have a similar electrochemical behaviour, precludes the development of anhydrous MoO_2 and MoO_3 in water above 200°C, as far as molar activities of 10^{-6} for the dissolved species are assumed. Nevertheless, the clear evidence of coloured products formation on the specimens exposed to the testing environments at 250°C suggested that the theoretical predictions of Ref. [10] are of limited use for describing properly the real situation. For instance, the hydrated forms of MoO_2 and MoO_3, not considered in the construction of the diagrams, but having Gibbs energies much lower than those of their relative anhydrous oxides at 25°C [11], are probably stable in water at 250°C, even though no data are available at high temperature to verify this hypothesis. Moreover, the formation of MoO_2 becomes thermodynamically possible by assuming higher activities for the dissolved substances than those used in Ref. [10].

Film growth on TZM as a result of corrosion in high temperature ($T > 150$°C) water is expected to follow the solid-state and solution diffusion models, widely accepted to explain the built-up of single or double oxide scales on a number of base-metals and their related alloys in similar environments [12–16]. The more or less protective properties of these layers determine the corrosion rate laws and are linked to the nature and morphology of the oxides, which depend strongly on the specific conditions and system employed.

As it emerged from XPS studies, the surface film characteristics and evolution observed on the samples exposed to deaerated and hydrogenated water on one hand and to oxygenated and hydrogen peroxide solutions on the other hand, present some similarities, which correlate reasonably with the comparable trends of their open circuit potentials and surface aspect from visual assessments. For these reasons, a common interpretation of TZM oxidation behaviour in each environmental couple has been attempted.

For reason of brevity, the discussion about the platinum electrochemical behaviour which has been detailed in a companion paper [2] can be summarized as follows: the experimental platinum voltages were compared to the theoretical equilibrium potentials of the redox couples, expected to dominate in either of the environmental testing conditions (see Table 3). The more or less satisfactory agreement found between the observed and calculated data was explained on the basis of thermodynamic and kinetic considerations and it was concluded that platinum could be reasonably taken as an indicator of the redox character of the environment.

4.1. Deaerated-hydrogenated water environments

By coupling the results of XPS analysis with the electrochemical data, it can be proposed that during the initial stage of TZM immersion, where the open circuit potential is still too low, a bilayered film of tetravalent Mo species develops probably from the inward diffusion of water (or oxygen-bearing ions from water) and the outward diffusion of metal-cations. The former produces an anhydrous dioxide, MoO_2, on the metal-side, through the overall redox reaction

$$Mo + 2H_2O = MoO_2 + 4H_{ads} \quad (1)$$

while the latter leads to an outer precipitate of oxyhydroxide $MoO(OH)_2$, according to

$$Mo = Mo^{4+} + 4e^- \quad \text{(metal-side)} \quad (2)$$

and

$$Mo^{4+} + 3H_2O = MoO(OH)_2 + 4H^+ \quad \text{(solution-side)} \quad (3)$$

coupled with

$$4H^+ + 4e^- = 4H_{ads} \quad \text{(metal or solution side)}. \quad (4)$$

The partial cathodic half reaction (Eq. (4)) (equivalent to water reduction, either deaerated or hydrogenated), which counterbalances TZM corrosion, is typically fast [17] because it is well catalyzed on metals and oxides and by polarizing the TZM interface near its equilibrium value, allows further thickening of the primary phases and the subsequent oxidation to higher valency either of the Mo^{4+} cations diffusing though the base layer or of the base layer itself. The progressive build-up of an outer hexavalent Mo oxide, in its hydrated form, H_2MoO_4, occurs by an oxidation-precipitation mechanism, according to the schema

$$Mo^{4+} + 4H_2O = HMoO_4^- + 2e^- + 7H^+. \quad (5)$$

coupled with

$$2H^+ + 2e^- = 2H_{ads}$$

and followed by

$$HMoO_4^- + H^+ = H_2MoO_4, \quad (6)$$

the overall process giving rise to acidification at the outermost solution/oxide interface. The attainment of a steady potential value indicates that at and beyond a transition time, further evolution of the layer does not produce substantial change of the corrosion rates. This situation, which appears to occur earlier in hydrogenated water and coincides with the XPS findings of a well defined bilayered inner Mo(IV)/outer Mo(VI) oxide structure, allows to suggest reasonably that, at steady potential, the outer hexavalent phase, once continuous over the inner one, controls TZM corrosion kinetics. Conversely, the results

relative to the samples exposed to deaerated water denote that longer immersion times are required in this case for ensuring an adequate coverage of the outer part with this protective species.

The proposed interpretation is also supported by the surface appearance of the specimens, which present the typical yellowish aspect of hydrated hexavalent Mo after exposure to hydrogenated water and independent of the contact time. In deaerated solution, where the oxidation kinetics is slower, they change from light purple (thin tetravalent Mo layer) to yellowish blue, as test duration increases and hexavalent Mo oxide becomes continuous and thickens over the underlying tetravalent phase.

An interpretation of the XPS findings concerning the Ti(IV)/(Mo(IV) + Mo(VI)) ratio, which does not vary with the exposure time and remains similar to the relative fraction of these elements in the bulk, can be attempted as follows: Mo and Ti from TZM oxidize non-selectively at the metal side giving rise to the inner oxide ($MoO_2 + TiO_2$) and to the ionic species $Mo^{4+} + Ti^{4+}$; their non-preferential outward diffusion produces the outermost layer, according to the proposed dissolution–precipitation mechanism for Mo^{4+} and probably by direct hydration for Ti^4, leading to the development of $H_2MoO_4 + TiO_2$. The Pourbaix diagram calculated for the Ti/H_2O system at 250°C indicates in fact that TiO_2 is the stable species in a wide range of pH and potentials including also the value at which oxidation of Mo(IV) to Mo(VI)) occurs [17].

4.2. Oxygenated-hydrogen peroxide solutions

The dominant cathodic processes involved as counterparts of TZM corrosion in oxygenated and hydrogen peroxide water solutions (see Table 3) are typically described to occur via a sequence of consecutive events involving adsorbed hydroxyl radicals as intermediates [17]. Both processes have been currently found to be irreversible (low exchange current density) on a number of metals and alloys as a consequence of their multistep character and have generally a solution-diffusion controlled kinetics. Accordingly, they do not work to pull the TZM corrosion potential near their equilibrium values, as it was the case for the more reversible couple H_2/H_2O through the half cathodic reaction (Eq. (3)), which, in turn, is probably hindered at the outer electrode surface for the presence of adsorbed OH^* radicals.

XPS data concerning the evolution with time of the individual Mo species, as a result of TZM exposure to oxygenated and hydrogen peroxide solutions, appear quite ambiguous and do not agree with the predictions derived from electrochemical data. In fact, at the very cathodic and constant potential values recorded throughout the entire test duration (see Tables 1 and 2), only low or intermediate valency oxides (or hydroxides) should develop, while the built-up of an outermost hexavalent phase is not expected. Moreover the film stoichiometry evolution, showing an increase with exposure time of the Mo(IV)/Mo(VI) ratio does not correlate with any common model of film evolution under constant open circuit potential. These considerations suggest that the formation of hexavalent Mo results probably from air oxidation of tetravalent Mo within the times elapsed before XPS analysis. This hypothesis accounts also for the greater Mo(VI) content, found on specimens M3 and M4, since they suffered longer atmospheric exposure, compared to specimens M33 and M44.

In the light of the integrated results, it could be therefore reasonably forwarded that film growth in water containing either oxygen or hydrogen peroxide gives rise to a poorly protective duplex layer of tetravalent Mo oxide and hydroxide according to Eqs. (1)–(4), which reaches quickly a limiting thickness as the overall rate of film formation balances that of its oxidative dissolution via reaction

$$MoO(OH)_2 = MoO(OH)_2^+ + e^- \quad \text{(solution side)} \qquad (7)$$

coupled with the proper dominant cathodic process according to water chemistry (see Table 3).

The anodic excursion of the potential in hydrogen peroxide solutions, related to the variation of concentration from 2.10^{-5} to 2.10^{-4} M/l during each chemistry transient, may give rise to a periodic increase of the $MoO(OH)_2^+$ concentration at the TZM interface and to the cyclic achievement of the precipitation conditions for Mo pentoxide/hydroxide, $MoO(OH)_3$, with no protective improvement of the base layer. The interpretation earlier formulated correlates also with the appearance of the specimen surfaces, showing the black purple colour of tetravalent Mo as a result of immersion in oxygenated water and the dark colour of $MoO(OH)_3$ produced in hydrogen peroxide solution in the form of a black and poorly adhering deposit from which particles continually spall. In this last case, the observed severe attack of the underneath metal suggests also that the layer produced in this environment reaches periodically a critical thickness for breakdown, leading to solution penetration and direct corrosion at the oxide/metal interface.

According to the proposed model (assuming equal rates for the competing processes of Mo(IV) oxide formation and dissolution) and bearing in mind the insoluble character of TiO_2, as predicted by theory [10], some Ti enrichment in the layer is expected, as found on specimen M4. The perfect matching between the relative Ti content in the film and in the bulk alloy found in the other cases appears quite doubtful. Arguments such as the preferential oxidation at cathodic potential of Mo compared to Ti on the metal side may be forwarded, but the reasons of an exact compensating effect is difficult to assess at least on the basis of the information deriving from the present study.

5. Conclusions

XPS studies conducted on TZM samples exposed to typical divertor coolant environments have made it possi-

ble to identify the main species present on the surfaces as corrosion products:

— The films formed in deaerated and hydrogenated water exhibited a bi-layered structure, comprising tetravalent and hexavalent Mo oxides and hydroxides in their inner and outer regions, respectively. The ratio between Mo(VI) and Mo(IV) was found to increase with immersion time, while the fraction of tetravalent Ti in TiO_2, also revealed in the layers, remained almost constant compared to the total amount of cationic species (Mo(IV) + Mo(VI) + Ti(IV)) and was similar to that of this metallic element in the alloy.

— TZM samples, after exposure to oxygenated and hydrogen peroxide solutions, were covered with tetravalent and hexavalent Mo oxides and hydroxides. The additional peak, found in the spectra from the samples exposed to hydrogen peroxide solution, was attributed to the intermediate Mo pentoxide. The fraction of Ti as TiO_2 in the layer formed in this last environment at short exposure time was higher than that of the substrate, contrarily to the other cases, where the concentrations of cationic Ti in the films reflected the composition of the bulk alloy.

The results from XPS characterization were subsequently used in connection with the open circuit potential data to formulate hypotheses about the electrochemical behaviour of TZM in the various environments considered in this study:

— It was suggested that the exposure of the TZM alloy to deaerated and hydrogenated water gave rise to the development, simultaneously on the metal side and electrolyte side, of a barrier-type, double-layered oxide/hydroxide, comprising Mo(IV) and Mo(VI) in its inner and outer parts, respectively. The passivating properties of this layer were attributed to the outer hexavalent Mo phase.

— It was proposed that the film produced on the TZM surface during immersion in oxygenated and hydrogen peroxide solutions, included only lower and intermediate valency Mo oxides/hydroxides, poorly protective. The presence of hexavalent Mo was thought to derive from air oxidation of these compounds during atmospheric exposure.

References

[1] M.F. Maday, J. Nucl. Mater. 233–237 (1996) 1397.
[2] M.F. Maday, Low cycle fatigue behaviour of TZM Mo-alloy in divertor water coolant, RT/INN/95, 1995.
[3] E. Zolti, PLANSEE-TZM, a High Temperature Molybdenum Alloy, private communication (June 1993).
[4] P.M.A. Sherwood, in: Practical Surface Analysis, eds. D. Briggs and M.P. Seah (Wiley, Chichester, 1985) p. 445.
[5] B. Brox, I. Olefjord, Surf. Interface Anal. 13 (1988) 3.
[6] R.A. Walton, J. Less Common Met. 54 (1977) 71.
[7] E. De Vito, P. Marcus, Surf. Interface Anal. 19 (1992) 403.
[8] W.E. Swartz Jr., D.M. Hercules, Anal. Chem. 43 (1971) 13.
[9] E. Destombes, N. Zoubov, M. Pourbaix, Comportement electrochimique du molybdène. Diagramme d'equilibres tension-pH du système Mo-H_2O à 25°C, Rapport technique RT 35 of CEBELCOR, 1956.
[10] J.B. Lee, Corros. NACE 37 (1981) 467.
[11] W.M. Latimer, The Oxidation States of the Elements and Their Potentials in Aqueous Solutions, 2nd Ed. (Prentice-Hall, New York, 1952) p. 250.
[12] Sato, Corros. Sci. 31 (1990) 1.
[13] J. Robertson, Corros. Sci. 29 (1989) 1275.
[14] J. Robertson, Corros. Sci. 32 (1991) 443.
[15] L. Tomlinson, Corros. NACE 37 (1981) 591.
[16] N.S. McIntyre, D.G. Zetaruk, D. Owen, J. Electrochem. Soc. 126 (1979) 750.
[17] D.D. Macdonald, M. Urquidi-Macdonald, Corros. NACE 46 (5) (1990) 380.